Transient Growth in Exactly Counter-Rotating Couette–Taylor Flow

Hristina Hristova and Sebastien Roch

Ecole Polytechnique de Montreal C.P. 6079, succ. Centre-ville Montreal (Qc) H3C 3A 7
and
Ecole Polytechnique, 91128 Palaiseau, France

Peter J. Schmid

Department of Applied Mathematics, University of Washington,
Box 352420, Seattle, WA 98195, U.S.A.
and
Laboratoire pour l'Hydrodynamique à l'Ecole Polytechnique (LADHYX-CNRS),
91128 Palaiseau, France

Laurette S. Tuckerman

Laboratoire d'Informatique pour la Mécanique et les Sciences de l'Ingénieur (LIMSI-CNRS),
B.P. 133, 91403 Orsay, France
and
Ecole Polytechnique, 91128 Palaiseau, France

Abstract. Transient growth due to non-normality is investigated for the Couette–Taylor problem with counter-rotating cylinders as a function of aspect ratio η and Reynolds number Re. For all $Re \leq 500$, transient growth is enhanced by curvature, i.e. is greater for $\eta < 1$ than for $\eta = 1$, the plane Couette limit. For fixed $Re > 130$, it is found that the greatest transient growth is achieved for η on the linear stability boundary. Transient growth is approximately 20% higher near the Couette–Taylor linear stability boundary at $Re = 310$, $\eta = 0.986$ than at $Re = 310$, $\eta = 1$, near the threshold observed for transition in plane Couette flow. For $106 < Re < 130$, the greatest transient growth occurs for a value of η between the linear stability boundary and one. For $Re < 106$, the flow is linearly stable and the greatest transient growth occurs for a value of η less than one. The energy in the optimal inputs is primarily meridional; that in the optimal outputs is primarily azimuthal. Pseudospectra are calculated for two contrasting cases.

1. Introduction

The transitions and patterns in Couette–Taylor flow are very well explained by linear stability theory. Indeed, this flow was historically used as a test case for linear stability theory. In contrast, transition in plane Couette

flow is unexplained to this day, remaining linearly stable at all Reynolds numbers despite the experimentally and numerically observed transition to turbulence. Because of this discrepancy, various mechanisms for transition have been proposed which bypass classical linear stability theory. All of these theories involve streamwise vortices, analogous to the Taylor vortices which become linearly unstable in Couette–Taylor flow.

One major line of research in plane Couette and other channel flows has focused on the effect of non-normality in the linearized evolution operator, which can enable large transient growth prior to eventual exponential decay (Butler and Farrell, 1992; Trefethen *et al.* 1993; Reddy *et al.*, 1993; Reddy and Henningson, 1993; Schmid and Henningson, 2001). This point of view has been only rarely applied to Couette–Taylor flow (Gebhardt and Grossmann, 1993; Meseguer, 2002), probably because classical linear stability theory is so successful in this case. However, in addition to the single non-dimensional parameter – the Reynolds number – of plane Couette flow, Couette–Taylor flow is characterized by two other parameters measuring curvature and Coriolis effects, providing a means of tuning the non-normality of the system.

Approaching the instability of plane Couette flow via Couette–Taylor flow is an appealing idea and has inspired a number of investigations (Nagata, 1998; Faisst and Eckhardt, 2000; Prigent and Dauchot, 2002). Our investigation proceeds somewhat in the opposite direction, taking a concept which has been extensively used in studying plane Couette flow and applying it to Couette–Taylor flow.

2. Methods

The Navier–Stokes equations are linearized about the Couette solution $\mathbf{U} = U_C(r)\underline{e}_\theta$, which is given by

$$U_C(r) = Ar + \frac{B}{r}, \tag{1a}$$

$$A = \frac{\mu - \eta^2}{2\eta(1 + \eta)}, \qquad B = \frac{2\eta(1 - \mu)}{(1 - \eta)(1 - \eta^2)}. \tag{1b}$$

Here $\eta \equiv r_{\text{in}}/r_{\text{out}}$ and $\mu \equiv \Omega_{\text{out}}/\Omega_{\text{in}}$, where r_{in}, r_{out}, Ω_{in}, Ω_{out} are the inner and outer cylindrical radii and angular velocities. Distances have been non-dimensionalized by $(r_{\text{out}} - r_{\text{in}})/2$ and velocities by $r_{\text{in}}\Omega_{\text{in}}$, so that $Re = r_{\text{in}}\Omega_{\text{in}}(r_{\text{out}} - r_{\text{in}})/(2\nu)$ where ν is the kinematic viscosity. This definition of Re, chosen for compatibility with the plane Couette convention for the case $\mu = -1$, differs by a factor of two from the conventional definition employed in Couette–Taylor flow, as do the expressions for A and B. The average radius is $\bar{r} = (1 + \eta)/(1 - \eta)$, so that the narrow-gap limit $\eta \to 1$ corresponds to $\bar{r} \to \infty$.

The Couette–Taylor geometry and the Couette solution are homogeneous in the azimuthal (θ) and axial (z) direction, which are analogous to the streamwise ($x \sim r\theta$) and spanwise (z) directions in plane Couette flow. Solutions to the linearized Navier–Stokes equations which are spatially bounded are therefore trigonometric in each of these directions, with wave numbers m and β.

$$(u_r, u_\theta, u_z) = (\hat{u}_r, \hat{u}_\theta, \hat{u}_z)(r, t) \exp(\mathrm{i}m\theta + \mathrm{i}\beta z). \tag{2}$$

The perturbations $(\hat{u}_r, \hat{u}_\theta, \hat{u}_z)$ are represented as 20-term series of Chebyshev polynomials in $y \equiv r - \bar{r}$, which are evaluated at the Gauss–Lobatto points.

The parameter space is too vast to permit full exploration. In this study we limit ourselves to $m = 0$, $\beta = \pi/2$, and $\mu = -1$ and we vary η between 0.5 and 1. The choice $m = 0$ of axisymmetric perturbations is made for simplicity but can be partially justified by previous studies. In plane Couette flow ($\eta = 1$), the transient growth achieved by streamwise-independent perturbations is, while not maximal, very close to the optimal value (Butler and Farrell, 1992; Trefethen *et al.*, 1993; Reddy and Henningson, 1993; Schmid and Henningson, 2001). The linear instability undergone by Couette–Taylor flow with counter-rotating cylinders is usually non-axisymmetric and leads to spirals, but its threshold and growth rate are close to those associated with the most unstable axisymmetric perturbation (Krueger *et al.*, 1966; Langford *et al.*, 1988). For a narrow gap, the choice $\beta = \pi/2$ is at most 20% smaller than the axial wave number corresponding to linear instability (Krueger *et al.*, 1966). We choose $\mu = -1$ so that the average angular velocity, i.e. the net Coriolis effect, vanishes. In contrast, Meseguer (2002) has investigated a range of values of μ for a fixed radius ratio $\eta = 0.88$ and has calculated m and β values which maximize the transient growth.

The full evolution equation is written symbolically as

$$\frac{\partial}{\partial t}\mathbf{u} = -\mathrm{i}\mathcal{L}\mathbf{u}. \tag{3}$$

As a measure of growth, we use the energy norm defined by

$$E(\mathbf{u}) = \|\mathbf{u}\|_{\mathrm{E}}^2 = \underbrace{\int\limits_{r=\bar{r}-1}^{\bar{r}+1} \left(|\hat{u}_r|^2 + \frac{1}{\beta^2 r^2}\left|\frac{\mathrm{d}}{\mathrm{d}r}(r\hat{u}_r)\right|^2 + \frac{m^2}{\beta^2 r^2}|\hat{u}_\theta|^2 \right) r\,\mathrm{d}r}_{E_{r,z}} + \underbrace{\int\limits_{r=\bar{r}-1}^{\bar{r}+1} |\hat{u}_\theta|^2\, r\,\mathrm{d}r}_{E_\theta}. \tag{4}$$

The maximal energy growth at time t for $\mathbf{u}$ evolving according to (3) is defined by

$$G(t) \equiv \sup_{\|\mathbf{u}(0)\|_{\mathrm{E}}^2 \neq 0} \frac{\|\mathbf{u}(t)\|_{\mathrm{E}}^2}{\|\mathbf{u}(0)\|_{\mathrm{E}}^2} = \|\exp(-\mathrm{i}\mathcal{L}t)\|_{\mathrm{E}}^2 \tag{5}$$

and is given by the square of the largest singular value $\sigma_{\max}$ under the energy norm of the operator $\exp(-\mathrm{i}\mathcal{L}t)$. The optimal transient growth is

$$G_{\max} = \sup_{t}\ G(t). \tag{6}$$

For operators which are linearly unstable, $G_{\max} = \infty$. The time for optimal growth $t_{\max}$ is that which achieves the maximum (sup) in (6). The optimal input, denoted by $\mathbf{u}(0)$, is the normalized initial condition which achieves the maximum (sup) in (5) and (6). The optimal output, denoted by $\mathbf{u}(t_{\max})$, is the velocity field resulting from the linearized Couette–Taylor evolution (3) starting from $\mathbf{u}(0)$.

A non-normal operator $\mathcal{L}$ is also characterized by its ϵ-pseudospectra $\Lambda_\epsilon(\mathcal{L})$, the sets of complex values z such that $\sigma_{\min}(zI - \mathcal{L}) \leq \epsilon$ (Trefethen *et al.*, 1993). For a normal operator, the ϵ-pseudospectrum is the union of the balls of radius ϵ surrounding each eigenvalue. For a non-normal operator, the ϵ-pseudospectrum may be much larger, especially surrounding certain eigenvalues deemed more responsible for non-normality.

Our codes for discretizing the Couette–Taylor operator were constructed by modifying the Matlab code for plane Couette flow written by Reddy (Reddy *et al.*, 1993; Reddy and Henningson, 1993) and published in
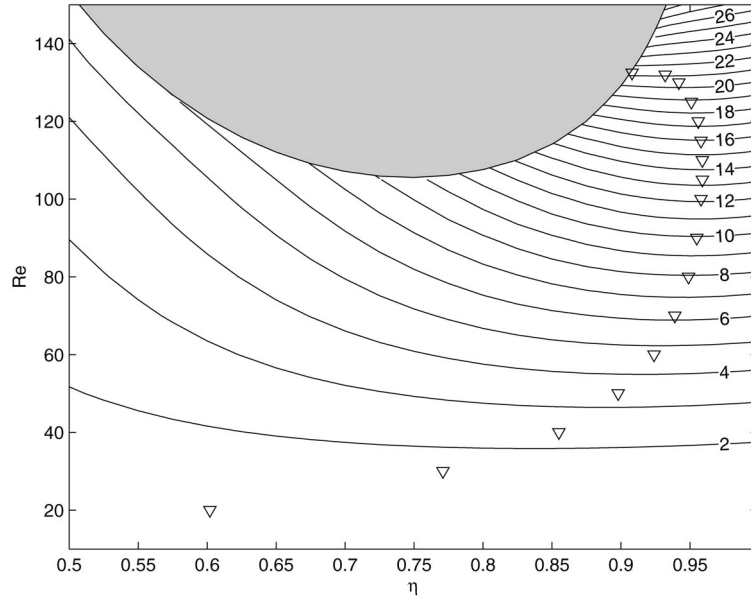

Figure 1. Contours of optimal growth for Couette–Taylor flow in the (η, Re) plane. Shaded area indicates the region of linear instability. Triangles indicate $\eta_{\mathrm{opt}}(Re)$, the value of η at which maximum growth is attained for a given value of Re.
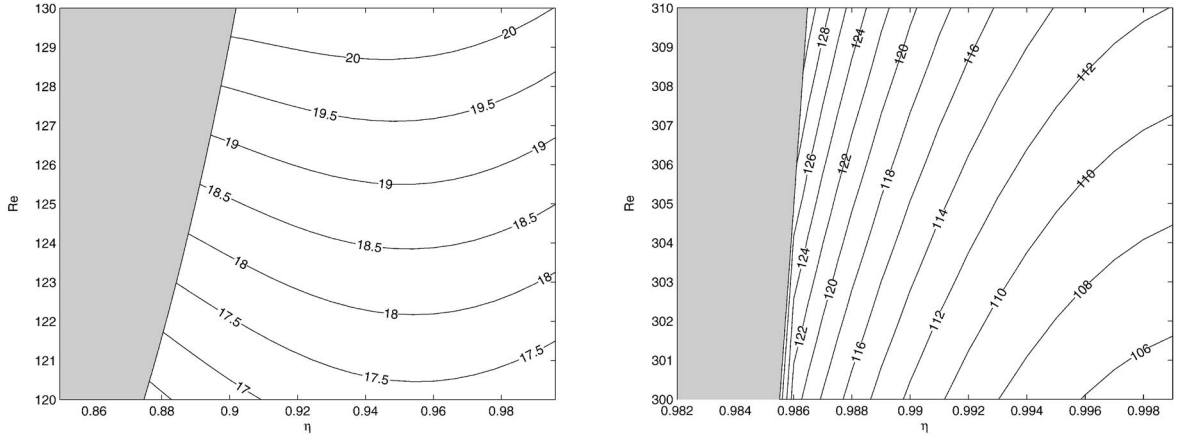
Figure 2. Left: contours of optimal growth $G_{\max}$ for $120 < Re < 130$, showing existence of optimal values $\eta_{\mathrm{opt}}(Re)$ between $\eta_{\mathrm{L}}(Re)$ and 1. Right: contours of optimal growth $G_{\max}$ for $300 < Re < 310$, showing rapid increase of $G_{\max}$ as η is decreased to the linear stability boundary.
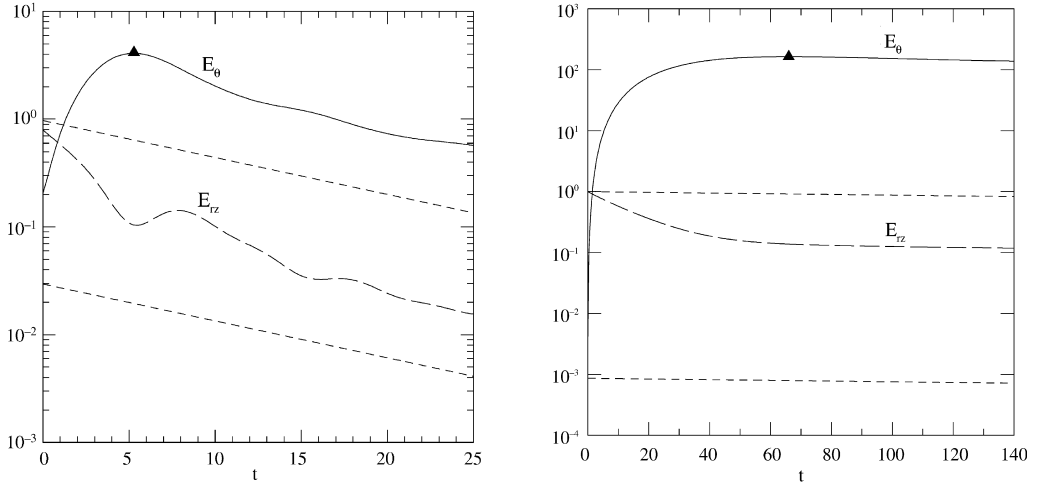

Figure 3. Left: time evolution of optimal input and of least stable eigenvector for $\eta = 0.50$, $Re = 125$. Solid and long-dashed curves represent $E_\theta(t)$ and $E_{r,z}(t)$, respectively, for optimal input. Higher and lower short-dashed curves represent $E_\theta(t)$ and $E_{r,z}(t)$, respectively, for least stable eigenvector. Triangle corresponds to $t_{\max}$. Right: time evolution of optimal input and of least stable eigenvector for $\eta = 0.99$, $Re = 350$.

Schmid and Henningson (2001). They were tested by comparing critical Reynolds numbers with published values (Krueger *et al.*, 1966). For computing the pseudospectra, we used the code `Eigtool` (formerly `PSAGUI`) written by (Wright and Trefethen, 2001), which implements the algorithm developed by Trefethen (1999) and available on the Web (Wright, 2002).

3. Results

Figure 1 shows the contours of constant optimal growth $G_{\max}$. Inside the shaded region, Couette flow is linearly unstable to axisymmetric perturbations. The boundary of this region is the critical Reynolds number $Re_{\mathrm{L}}(\eta)$. $Re_{\mathrm{L}} \to \infty$ as $\eta \to 1$, as expected since plane Couette flow is linearly stable for all Reynolds numbers. We may also consider the rightmost portion of the linear stability boundary as a function $\eta_{\mathrm{L}}(Re)$.

Our main result is that the maximum growth for a fixed Reynolds number, indicated by the triangles in Figure 1, is always achieved for a radius ratio $\eta = \eta_{\mathrm{opt}}(Re)$ which is less than one. Thus, curvature increases singular values (transient growth) just as it does eigenvalues (exponential growth). This optimal
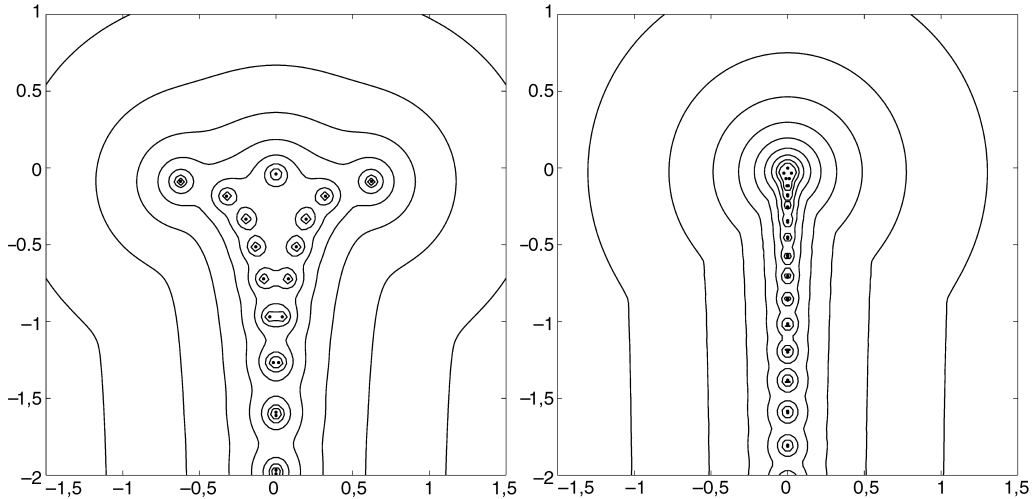
Figure 4. Left: pseudospectra for Couette–Taylor flow for $\eta = 0.5$ and $Re = 125$. Contours correspond to $\epsilon = 10^{-1.8}, 10^{-1.5}, \ldots, 10^{0}$. Right: pseudospectra for Couette–Taylor flow for $\eta = 0.99$ and $Re = 350$. Contours correspond to $\epsilon = 10^{-2.4}, 10^{-2.1}, \ldots, 10^{0}$.

value increases with Reynoldsnumber to a maximum of $\eta_{opt} \approx 0.96$ for $Re \approx 110$, and then abruptly decreases and terminates by meeting the linear instability boundary $\eta_L \approx 0.9$ at $Re \approx 130$. For $Re \leq 130$, the optimal growth does not exceed a factor of 21; see Figure 2. For $Re > 130$, the maximum growth is achieved for η at $\eta_L(Re)$. Arbitrarily high values of G_{max} can be attained by increasing Re, since for plane Couette flow, i.e. $\eta = 1$, it is known that $G_{max} \sim Re^2$ (Trefethen *et al.*, 1993; Reddy and Henningson, 1993; Schmid and Henningson, 2001). In fact G_{max} is approximately 20% higher for $\eta = \eta_L$ than for $\eta = 1$ over the range $300 < Re < 310$, the approximate threshold for transition to turbulence in plane Couette flow; see Figure 2.

We have studied in detail two contrasting cases: $\eta = 0.5$, $Re = 125$ and $\eta = 0.99$, $Re = 350$. In the first case, $\eta = 0.5$ or equivalently $\bar{r} = 3$, curvature plays an important role. The second case, $\eta = 0.99$ or equivalently $\bar{r} = 199$, is very near the plane Couette limit. The Reynolds numbers have been chosen to be close to the linear instability threshold Re_L in each case.

The optimal inputs $\mathbf{u}(0)$ are concentrated primarily in the meridional components (u_r, u_z) with a very small azimuthal component u_θ; for the optimal outputs $\mathbf{u}(t_{max})$, the situation is reversed. This evolution corresponds to the generation of streaks – deformations of the azimuthal velocity profile – by the vortices. This physical process is believed to be a key element in the transition to turbulence in plane Couette flow. Figure 3 shows the evolution in time of the energies in the azimuthal component E_θ and in the meridional components $E_{r,z}$ starting from the optimal inputs $\mathbf{u}(0)$ and from the least stable eigenvectors.

Figure 4 shows the spectrum and pseudospectra of the operators $\mathcal{L}$. Both pseudospectra plots contain contours (for the smaller values of ϵ) surrounding individual eigenvalues and bulb-shaped contours (for the larger values of ϵ) surrounding the entire spectrum. Since the spectrum for $\eta = 0.99$, $Re = 350$ is quite localized on the imaginary axis, bulb-shaped pseudospectral contours in this case are an indication that non-normal effects are most pronounced for eigenvalues near the origin.

Acknowledgment

References

Butler, K.M., Farrell, B.F. (1992). Three-dimensional optimal perturbations in viscous shear flow. Phys. Fluids A **4**, 1637–1649.

Faisst, H., Eckhardt, B. (2000). Transition from the Couette–Taylor system to the plane Couette system. *Phys. Rev. E*, **61**, 7227–7230.

Gebhardt, T., Grossmann, S. (1993). The Taylor–Couette eigenvalue problem with independently rotating cylinders. *Z. Phys. B*, **90**, 475–490.

Krueger, E.R., Gross, A. DiPrima, R.C. (1966). On the relative importance of Taylor-vortex and non-axisymmetric modes in flow between rotating cylinders. *J. Fluid Mech.*, **24**, 521–538.

Langford, W.F., Tagg, R., Kostelich, E.J., Swinney, H.L., Golubitsky, M. (1988). Primary instabilities and bicriticality in flow between counter-rotating cylinders. *Phys. Fluids*, **31**, 776–785.

Meseguer, A. (2002). On the nonnormal effects in the Taylor–Couette problem. *Theoret. Comput. Fluid Dynamics*, **16**, ■–■.

Nagata, M. (1998). Tertiary solutions and their stability in rotating plane Couette flow. *J. Fluid Mech.*, **358**, 357–378.

Prigent, A., Grégoire, G, Chaté, H., Dauchot, O., van Sarloos, W. (2002). Large-scale finite-wavelength modulation within turbulent shear flows. *Phys. Rev. Lett.*, **89**, 014501.

Reddy, S.C., Henningson, D.S. (1993). Energy growth in viscous channel flow. *J. Fluid Mech.*, **252**, 209–238.

Reddy, S.C., Schmid, P.J., Henningson, D.S. (1993). Pseudospectra of the Orr–Sommerfeld operator. *SIAM J. Appl. Math.*, **53**, 15–47.

Schmid, P.J., Henningson, D.S. (2001). *Stability and Transition in Shear Flows*. Springer-Verlag, New York.

Trefethen, L.N., Trefethen, A.E., Reddy, S.C., Driscoll, T.A. (1993). Hydrodynamic stability without eigenvalues. Science **261**, 578–584.

Trefethen, L.N. (1999). Computation of pseudospectra. *Acta Numeri.*, **8**, 247–295.

Wright, T.G. Trefethen, L.N. (2001). Large-scale computation of pseudospectra using ARPACK and Eigs. *SIAM J. Sci. Comp.* **23**, 591–605.

Wright, T.G. (2002). `www.comlab.ox.ac.uk/pseudospectra/ergtool`.